Multicode turbulence simulations of diverted TCV plasmas and detailed validation against the experiment

D. S. Oliveira[1], T. Body[2], D. Galassi[1], C. Theiler[1], E. Laribi[3], P. Tamain[3], A. Stegmeir[2], P. Ricci[1], Zholobenko[2], M. Giacomin[1], H. Bufferand[3], J. A. Boedo[4], G. Ciarolo[3], C. Colandre[1], H. Oliveira[1], G. Fourestey[5], S. Gorno[1], F. Imbeaux[3], F. Jenko[2], V. Naulin[6], N. Offeddu[1], H. Reimerdes[1], E. Serre[7], C. K. Tsui[1], N. Varini[5], N. Vianello[8], M. Wiesenberger[6], C. Wüthrich[1] and the TCV Team*

[1]*Swiss Plasma Center, École Polytechnique Fédérale de Lausanne (EPFL), Lausanne, Switzerland;* [2]*Max Planck Institute for Plasma Physics, Garching bei Müchen, Germany;* [3]*CEA,IRFM, Saint Paul-lez-Durance, France;* [4]*University of California, California, USA;* [5]*Scientific IT and Application Support (SCITAS), Lausanne, Switzerland;*[6]*Department of Physics, Technical University of Denmark, Kgs. Lyngby, Denmark;* [7]*Aix Marseille Université, Marseille, France;*[8]*Consorzio RFX, Padova, Italy;*

This contribution presents preliminary results of the validation of state-of-the-art turbulence codes against well-diagnosed experiments in the TCV tokamak. The simulations were carried out by GBS, GRILLIX, and TOKAM3X codes for a Lower Single-Null (LSN) L-mode attached TCV plasma and, for the first time, in realistic size. The scenario depicted in the simulations was developed in the TCV tokamak and was optimized for this validation exercise. In the following, the level-of-agreement and comparisons of selected profiles are discussed.

Experimental Reference Scenario: TCV-X21

The TCV-X21 scenario developed in the TCV tokamak is a LSN L-mode Ohmic plasma with $I_p = 160 - 170kA$, line-averaged density $\langle n_e \rangle \sim 2.5 \times 10^{19}[m^{-3}]$, attached, and a $B_{tor} = 0.95T$. The magnetic geometry is shown in Fig.(1) together with the diagnostics employed in the construction of the dataset. The reduced B_{tor}, compared to the nominal $1.4T$, was conceived to reduce the computational costs, since all lengths in the codes are normalized by the ion sound Larmor radius. The impact of neutrals in the divertor region was minimized by fuelling the

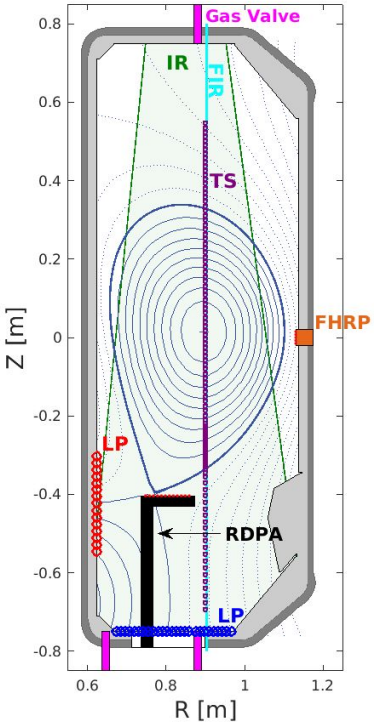

Figure 1: Magnetic geometry and diagnostics: Langmuir Probes (LP), Reciprocating Divertor Probe Array (RDPA), Thomson Scattering (TS), Fast Horizontal Reciprocating Probe (FHRP), Infrared Camera (IR).

*See author list of S. Coda et al. Nucl. Fusion 59 112023

plasma from the top (see Fig.1), since they are not included in the simulations.

Simulations of the TCV-X21 scenario

The GBS [1], GRILLIX [2] and TOKAM3X [3] codes evolve two fluid, drift-reduced Braginskii equations for the basic fluid variables, the electrostatic potential ϕ and the generalized vorticity ω. In GBS simulations, the resistivity $\eta_{||}$ is multiplied by 3 and the heat conductivity (for electrons and ions $\chi_{e;i,||}$) divided by 20 to avoid numerical instabilities. In TOKAM3X, $\eta_{||}$ and $\chi_{e;i,||}$ are, respectively, multiplied and divided by 1.8 due to the rescaling of the normalization parameters. The simulations for the TCV-X21 case do not include neutrals; a ring-shaped n source located just inside the confined plasma mimics the ionization. Similarly, the T_e source consists of a circular-shaped region centered in the plasma core. For GBS, the source strengths are estimated using the scaling law introduced in Ref.[1], and tuned to approximately match the density and temperature at the separatrix as measured with TS (see Fig.1). Similarly for TOKAM3X. For GRILLIX, the n source is set to match the n experimental value at the separatrix and no T_e source is used, but instead the power crossing the separatrix obtained from the experiment. GBS adopts Bohm boundary conditions (BC), while GRILLIX and TOKAM3X adopt a Bohm-Chodura BC, with the first including the condition that ions are only allowed to flow out of the simulation grid. GRILLIX and TOKAM3X use flux-aligned grids, while GBS uses a fully non-aligned discretization.

Experiment-Simulation Comparisons

The preliminary results for the validation in forward B-field shown below applied *rigorously* the metric presented in [4]. Here we limit the discussion in terms of d_j, the weighted distance between the experiment and the simulation profiles, and $\chi \in [0,1]$, the overall level-of-agreement, calculated including all observables present in the dataset (which will be presented in [5]). Perfect agreement is indicated by $d_j = 0$ and $\chi \sim 1$, and clear disagreement by $d_j \gg 1$ and $\chi = 1$.The quantitative agreement at the outerboard midplane (OMP) with the fast reciprocating probe measurements is $\chi_{OMP} = 0.58 - 0.65$. This is at the limit between agreement-disagreement.However, since error bars for the simulations are not included in this work, a value of χ showing a poor agreement is expected. Figs.(2.A-C) shows a fair agreement between the codes and the experimental profiles of n and T_e, despite the GBS and TOKAM3X broader profiles. This is confirmed in the table on the right of Fig.(2), which shows larger fall-off lengths for the simulations than in the experiment. For GBS and TOKAM3X, this is attributed to the relaxed values of $\eta_{||}$ and $\chi_{e;i,||}$. It is important to note that T_e shows the best agreement value, but this is also related to the large error bars. Fig.(2.B) shows that the codes have different predictions

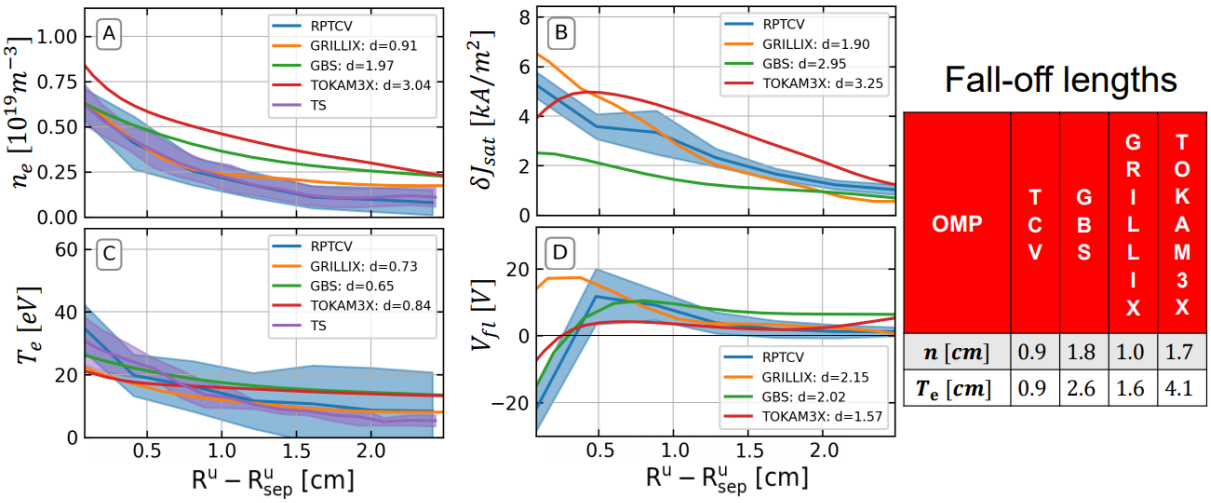

Fall-off lengths

OMP	TCV	GBS	GRILLIX	TOKAM3X
$n\ [cm]$	0.9	1.8	1.0	1.7
$T_e\ [cm]$	0.9	2.6	1.6	4.1

Figure 2: (*right*) Profiles of n_e, T_e, V_{fl}, and δJ_{sat} measured at the OMP by the FHRP. (*left*) Table showing the fall-off length estimated from the experiment and the codes. The purple profiles are measured by TS.

for δJ_{sat}: underestimation in GBS, overestimation in GRILLIX and a non-monotonic behavior in TOKAM3X, which is caused by the proximity of the flux-aligned grid to the X-point. Fig.(2.D) shows that GBS closely match the experimental V_{fl} near the separatrix, while in the far-SOL, this is observed for GRILLIX. However, the best overall quantitative agreement is displayed by TOKAM3X (smallest d_j). At the LFS/HFS targets the agreement is overall rather poor;

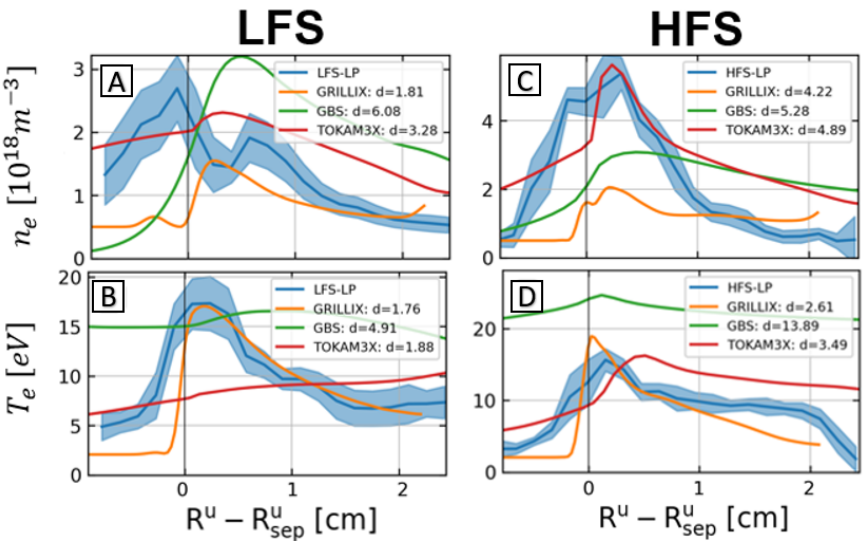

Figure 3: Low-field-side (LFS) and High-field-side (HFS) target profiles.

$\chi_{LFS-HFS} \sim 1$ for all codes. Figs.(3.A-D) show that the n and T_e profiles in the simulations have the same order as the experimental ones, but differ in shape. Target profiles can also be strongly affected by the BCs. This is the possible explanation for the underestimation of n profiles by GRILLIX. For GBS, n and T_e profiles are broader than the experimental ones in both targets, similar to the result at the OMP. Additionally, GBS simulations use Bohm BCs, hence not including drifts that might be relevant in this low n scenario. This is in accordance with the n profile predicted by TOKAM3X at HFS target, Fig.(3.D), which includes the $E \times B$ and the

∇B drifts in the BC and captures the experimental n peak. The δJ_{sat} at both targets (not shown here), for all codes, are $5-10$ times smaller than the experimental observation. This result is not limited to the targets as shown by Figs.(4.2.A-D) for the 2D profiles of δJ_{sat} in the divertor volume.

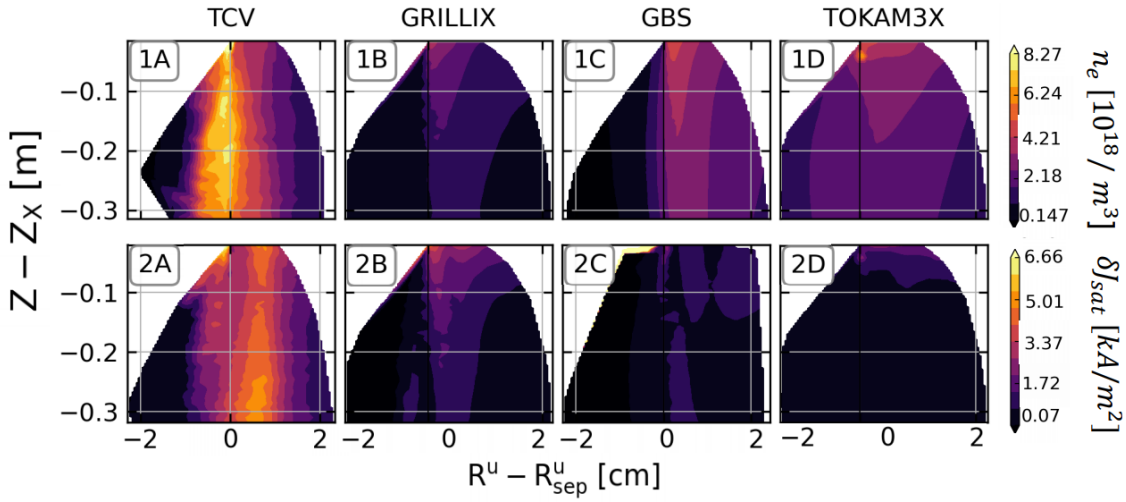

Figure 4: 2D Divertor volume profiles of n_e and δJ_{sat} measured by the RDPA.

Summary

In this work, the TCV-X21 scenario was developed and applied in a multi-code validation effort using GBS, GRILLIX, and TOKAM3X codes. The TCV-X21 is specially optimized to allow the first full-size turbulence simulations of an LSN L-mode attached plasma in TCV, in both field directions. An extensive dataset was also prepared for the validation exercise and a detailed discussion of the validation will be presented in Ref.[5]; here we limited to discuss preliminary results of selected profiles. We found a fair agreement at the OMP, $\chi_{OMP} = 0.58 - 0.65$, with the simulations reproducing the correct shape of the experimental profiles, but with larger fall-off lengths. The major discrepancies are in the divertor volume and at the targets, in particular, with respect of the fluctuation levels that are $5-10$ times below the experimental observation. In this context, the validation methodology is a powerful to assess the causes for such disagreement, indicating the direction of the future improvements in the codes.

References

[1] Giacomin et al. J. Plasma Phys., **47**, 2020

[2] Zholobenko et al. Plasma Phys. Control. Fusion., **63**, 2021

[3] Tamain et al. J. Comput. Phys., **47**, 2016

[4] Ricci et al. Phys. Plasma, **22**, 2015

[5] Oliveira and Body et al. Nuc. Fusion in prep, 2021